Published in final edited form as:
J Endocrinol. 2009 October ; 203(1): 65–74. doi:10.1677/JOE-09-0026.

Degradation of IRS1 leads to impaired glucose uptake in adipose tissue of the type 2 diabetes mouse model TALLYHO/Jng

Yun Wang, **Patsy M. Nishina**, and **Jürgen K. Naggert**
The Jackson Laboratory, 600 Main Street, Bar Harbor, ME, 04609

Abstract

The TALLYHO/Jng (TH) mouse strain is a polygenic model for type 2 diabetes characterized by moderate obesity, impaired glucose tolerance and uptake, insulin resistance, and hyperinsulinemia. The goal of this study was to elucidate the molecular mechanisms responsible for the reduced glucose uptake and insulin resistance in the adipose tissue of this model.

The translocation and localization of GLUT4 to the adipocyte plasma membrane were impaired in TH mice compared to control C57BL6/J (B6) mice. These defects were associated with decreased GLUT4 protein, reduced PI3 kinase activity and alterations in the phosphorylation status of IRS1. Activation of JNK 1/2, which can phosphorylate IRS1 on Ser307, was significantly higher in TH mice compared to B6 controls. IRS1 protein but not mRNA levels were found to be lower in TH mice than controls. Immunoprecipitation with anti-ubiquitin and western blot analysis of IRS1 protein revealed increased total IRS1 ubiquitination in adipose tissue of TH mice. SOCS1, known to promote IRS1 ubiquitination and subsequent degradation, was found at significantly higher levels in TH mice compared to B6. Immunohistochemistry showed that IRS1 co-localized with the 20S proteasome in proteasomal structures in TH adipocytes, supporting the notion that IRS1 is actively degraded.

Our findings suggest that increased IRS1 degradation and subsequent impaired GLUT4 mobilization play a role in the reduced glucose uptake in insulin resistant TH mice. Since low IRS1 levels are often observed in human type 2 diabetes, the TH mouse is an attractive model to investigate mechanisms of insulin resistance and explore new treatments.

Keywords

IRS1 degradation; adipose tissue; type 2 diabetes; mice

Introduction

Understanding the pathogenesis of type 2 diabetes (T2D) is necessary to identify therapeutic targets as well as to generate prognostic information, which ultimately should lead to improved outcomes in affected individuals (O'Rahilly, et al. 2005). The etiology of T2D likely involves genetic predisposition and non-genetic risk factors such as high calorie diets and reduced physical activity (O'Rahilly et al. 2005), (Leahy 2005). It is commonly held that most forms of T2D in human follow polygenic inheritances; i.e., predisposing alleles from multiple genes

Address correspondence to: Jürgen K Naggert Ph.D. The Jackson Laboratory, 600 Main Street, Bar Harbor, ME Tel.: 207-288-6382. Fax: 207-288-6077; Juergen.Naggert@jax.org.

Declaration of interest The authors have no conflicting interests to disclose.

contribute to the development of the disease. Further, T2D is genetically heterogeneous, and various pathologic pathways underlie the disease in different affected individuals (O'Rahilly et al. 2005), (Leahy 2005). Possibly owing to the etiological complexity, only recently have common molecular factors been identified that affect pathogenesis of human T2D (McCarthy and Zeggini 2007).

A hallmark of T2D is insulin resistance. During normal glucose homeostasis, insulin suppresses hepatic glucose production and increases glucose uptake in muscle and adipose tissues. The latter results from insulin induced translocation to the cell surface of glucose transporter 4 (GLUT4), the major insulin-responsive glucose transporter. Insulin binding to its receptor initiates a cascade of events resulting in translocation of GLUT4 from an intracellular compartment and insertion into the plasma membrane. The insulin resistance of T2D mellitus includes a blunting of the insulin-stimulated increase in glucose uptake into adipocytes and muscle. Decreased GLUT4 expression in adipocytes can affect glucose homeostasis (Minokoshi, et al. 2003) and adipose-selective targeting of the *Glut4* gene leads to impaired insulin action in muscle and liver (Abel, et al. 2001).

Low insulin receptor substrate 1(IRS1) expression and protein levels have been linked to the development of insulin resistance and T2D in humans (Carvalho, et al. 1999) and mice heterozygous for insulin receptor (IR) and IRS1 null alleles (Bruning, et al. 1997). Hirosumi et al. proposed that activation of c- Jun N-terminal kinase (JNK) leads to a reduction in IRS1 levels and thus to insulin resistance in the Lep^{ob} mouse and a diet induced obesity model (Hirosumi, et al. 2002). What factors activate this pathway and whether it is a general principle in T2D has not yet been fully established.

Genetic animal models have been valuable resources for T2D research, and several polygenic rodent models have been developed (Rees and Alcolado 2005). The TALLYHO/Jng (TH) mouse strain is a newly established polygenic model for T2D characterized by moderate obesity, impaired glucose tolerance and uptake, insulin resistance, hyperinsulinemia, and male limited hyperglycemia. The TH strain originated from phenodeviant mice with polyuria discovered in a colony of outbred Theiler Original mice (Kim, et al. 2001). Several phenodeviants were imported into The Jackson Laboratory and underwent inbreeding by an intercross/backcross scheme with selection for hyperglycemia in male mice. Although hyperglycemia initially segregated as a single recessive trait, subsequent mapping studies in backcrosses with B6 and CAST/Ei mice found several genetic loci contributing to hyperglycemia in the crosses with a major locus mapping to mouse chromosome 19 (Kim et al. 2001). To better validate the TH mouse as a model for human T2D, we examined GLUT4 protein levels, translocation and localization in adipose tissue, as well as components of the insulin signaling pathway. We show not only dysregulated GLUT4 translocation as in other T2D models (Farese, et al. 2007), but also a defect in phosphoinositide (PI) 3-kinase activation, and low IRS1 levels. We found that IRS1 localizes aberrantly to proteasomal structures in TH adipocytes. Our study identifies IRS1 degradation as a contributor to insulin resistance in TH mice.

Materials and Methods

Materials

Anti-IRS1 and Anti-phospho-S307 IRS1 antibodies were obtained from Cell Signaling Technology (Danvers, MA) and Santa Cruz Biotechnology (Santa Cruz, CA). IRS1 ELISA kits, the antibodies for phospho-tyrosine (anti-PY), and PI3K (p85) were purchased from Upstate (Lake Placid, NY). Anti-GLUT4 and Anti-SOCS1 antibodies were purchased from Abcam (Cambridge, MA). Anti-Ubiquitin antibodies were from Sigma (Saint Louis, MO). Anti-20S proteasome alpha/beta antibodies were obtained from Novus (Littleton, CO). Catch

and Release Kit for PI3 kinase assays were obtained from Upstate (Lake Placid, NY). Porcine insulin was purchased from Eli Lilly (Indianapolis, IN).

Animals

The TALLYHO/Jng (TH) inbred mouse strain has been described in previous studies (Kim et al. 2001), (Kim, et al. 2006). Ten to twelve week-old male TH mice were used in this study. Mice were bred and maintained in the Research Animal Facility at The Jackson Laboratory with free access to food (NIH31 diet with 6% fat) and water on a 12-h light: 12-h dark cycle. All animal studies were performed with the approval of The Jackson Laboratory Animal Care and Use Committee. Male C57BL6/J (B6) mice (10-12 week old) were used as normoglycemic controls as described (Kim et al. 2001),(Kim et al. 2006),(Sung, et al. 2005).

Real-time quantitative PCR

Real-time PCR assays were performed as previously described (Wang, et al. 2006) on an ABI PRISM 7500 SDS instrument. Samples were analyzed in triplicate in three independent runs. To quantify the gene expression profiles, we used the comparative threshold cycle method. PCR primers that amplified 150-180 bp fragments of mouse *Irs1* cDNA (NM010570) were used (F: CGCTACATCCCAGGTGCTAAC, R: GCGGAGTGAGTTCTCTTTCGA).

Immunhistochemistry and confocal microscopy

Immunohistochemical analyses were performed as described previously with modifications (Liu, et al. 1993). Briefly, mice were either fasted overnight and left untreated or allowed to eat ad lib and then given an intraperitoneal injection of glucose (1g/kg) and insulin (8 units/kg). 30 minutes after the injections the mice were anesthetized with tribromoethanol and perfused with phosphate buffered saline (PBS) followed by 4% paraformaldehyde (PFA) in PBS as fixative. Abdominal adipose tissue was removed and postfixed in the same fixative overnight at room temperature. A microwave procedure was used for antigen retrieval in paraffin-embedded tissue sections (8 min in citrate buffer, pH 6–6.5). Slides were then incubated in 0.3% hydrogen peroxide for 30 min to inhibit endogenous peroxidase activity. After incubation with blocking solution (3% normal goat serum), slides were incubated overnight with rabbit polyclonal antiserum against GLUT4 protein, mouse monoclonal anti IRS1 antibodies, and rabbit polyclonal anti-proteasome 20S alpha + beta antibodies. Confocal microscopy (Leica CTR6000, Germany) was used to detect GLUT4 distribution, and fluorescence microscopy (Leica DMLB, Germany) was employed for IRS1 and 20S proteasome protein localization. For single or double immunofluorescence staining, FITC and rhodamine-conjugated secondary antibodies were employed. Analysis and photo-documentation were described in our previous studies (Wang et al. 2006),(He, et al. 2000). The specificity of staining was confirmed using negative controls in which the primary antibody was omitted.

Immunoprecipitations and western blot analysis

Immunoprecipitations and western blot analyses of insulin signaling proteins were performed on abdominal adipose tissue homogenates as previously described (Araki, et al. 1994), (Hu, et al. 2004). Briefly, mice were fasted overnight and intraperitoneally injected with insulin (0.5 U/kg body wt) or saline. 30 minutes after injection, epididymal fat pads were dissected and saved for immunoprecipitation and immunoblot (IB) analysis of insulin signaling molecules. Adipose tissue samples were homogenized in buffer (50 mM Tris-HCl, 150 mM NaCl, 1 mM EDTA, 1% Triton X-100, 0.5% NP40, 0.1 mM Na_3VO_4 and protease inhibitors) and particulates removed by centrifugation. The supernatants were incubated overnight at 4°C with antibodies against IRS1, p85 or ubiquitin, followed by the addition of protein A or G-sepharose and antibodies against IRS1 and phospho-tyrosine. Immunoprecipitated proteins were resolved

by PAGE and detected by chemoluminescence after western blotting. Quantitative densitometric analyses of the chemoluminescence photographs were carried out on a LAS-1000 plus densitometer and IMAGE Gauge V3.45 software. Results were expressed as percentage of signal intensity seen in samples from insulin-stimulated B6 animals.

Phosphatidylinisitol (PI3) kinase activity assay

Mice were fasted overnight (18h) and then given insulin (0.5U/kg) or saline intraperitoneally. 30 minutes after injection, adipose tissue was homogenized on ice with a 5 mm Omni ultrasound probe. PI3K assays were performed as previously described (Farese et al.),(Krook, et al. 1997),(Storgaard, et al. 2001). Briefly, to 500 μl aliquots of diluted cell lysate (500 μg) in fresh tubes were added 4 μg of PY20 antibody and 10μl (1μg) of Antibody Capture Affinity Ligand (Fisher Scientific, Pittsburgh, PA). The samples were briefly mixed and incubated for 5-15 minutes at room temperature. Proteins were captured in an eppendorf spin column at 1,500 × g for 2 minutes. The spin columns were washed twice with 500 μl of 1X Catch and Release Lysis/wash buffer and centrifuged for 3 minutes at 2,000 × g. The bound protein was eluted with 500 μl of assay dilution buffer followed by 30-60μl of water to obtain final combined eluates. Phosphatidyl inositol (PI), 1mg/ml, was dispersed by sonication for 15 min in 5mM HEPES. PI was pre-incubated with the immunoprecipitates at 4°C for 20 min at a final conc. of 0.2 mg/ml. The phosphorylation reaction was started by adding 20μCi [gamma^{32}P]ATP and $MgCl_2$ to final conc. of 50μM ATP (cold) and 5mM $MgCl_2$ in a volume of 50 μl. After incubation for 20 min at 25°C the reaction was terminated by adding 100μl of 1M HCl. Phospholipids were extracted immediately with 200 μl $CHCl_3$/MeOH (1:1). The organic phase was washed with 80 μl MeOH/HCl (1:1) and 15μl of the organic phase were spotted onto a silica gel TLC plate. Phosphorylated products were separated by TLC in a $CHCl_3$/MeOH/4 M NH_4OH (9:7:2) developing solvent for 1 hour and visualized by autoradiography.

Measurement of JNK activation

The phosphorylation status at threonine 183 and tyrosine 185 of JNK1/2 was assayed using a commercial antibody bead kit for phospho-JNK1/2 [pTpY 183/185] (Cat. LHO0081, Biosource, Camarillo, CA).

Adipocyte isolation and glucose uptake

Adipocytes were isolated from overnight fasted mice by a protocol modified from Rodbell (Rodbell 1964). The epididymal fat pads were removed and minced into rice-sized pieces and then placed in pre-gassed (95% O_2, 5% CO_2) Krebs-Ringer buffer with HEPES (KRBH, 117mM NaCl, 4.72mM KCl, 2.5mM $CaCl_2$, 1.2mM KH_2PO_4, 1.2mM$MgSO_4$, 10mM $NaHCO_3$, 20mM HEPES, 200nM adenosine, filtered and adjusted to pH 7.4) with 3% BSA and 2.5mg/ml collagenase. The cells were incubated in a 37°C water bath for 1 hour with shaking at 100 rpm. After digestion, the cell suspension was passed through a pre-moistened 250μm filter and cells were washed three times with cold KRBH with 3% BSA. The diluted cell suspension was then dispersed equally by volume into 5mL cell culture tubes. Cells were treated with saline (basal) or 70nM insulin for 30 minutes before the addition of 0.2 μCi of 2-[^{3}H]-deoxyglucose. After 10 minutes, glucose uptake was stopped by centrifugation of the cells over dinonyl phthalate oil at 350 × g for 2 minutes. Cells were lysed with a 3% SDS (v/v) buffer and the lysates were solubilized in Ultima-Gold scintillation cocktail. Cytochalasin B was used as a control for non-insulin dependant glucose uptake. An aliquot of each cell lysate was taken prior to the addition of scintillation fluid and all counts were normalized for protein concentration. Final glucose uptake values are presented as pMol/mg/min (Zisman, et al. 2000).

Sub-cellular fractionation of isolated adipocytes

Mice were fasted for 4 hours after the dark period and then given insulin (0.5 U/kg) or saline by intraperitoneal injection. 30 minutes later, the epididymal adipose tissue was collected. Subcellular fractions were prepared as previously described (Tsuji, et al. 2001), with some modifications. In brief, the isolated adipocytes were suspended in 10 ml of homogenization buffer A (20 mM Tris-HCl, 1mM EDTA, 255 mM sucrose, pH7.4) with protease inhibitors. They were homogenized on ice and were centrifuged at 5,000 × g for 5 min at 4°C to remove fat droplets. The homogenates were centrifuged for 20 min at 19,000 × g. The initial supernatant contained the microsomal membrane fraction. The plasma membrane-rich (PM) fractions were prepared as follows: the initial pellet was re-suspended in 3 ml buffer B (20mM Tris-HCl, 1mM EDTA, pH 7.4 with protease inhibitors), then layered onto a 6 ml sucrose cushion (38% sucrose in Buffer B) and centrifuged at 100,000 × g for 70 min. The PMs, collected at the interface on top of the sucrose cushion were resuspended in buffer B and centrifuged at 40,000 × g for 20 min and yielded a pellet of the plasma membrane fraction. The 100,000 × g pellet was re-suspended by homogenization in buffer A, yielding the mitochondrial and nuclear fractions. The 19,000 × g initial supernatant was centrifuged for 20 min at 41,000 × g, yielding a pellet of the high-density microsome (HDM) fraction. The 41,000 × g supernatants were centrifuged at 180,000 × g for 70 min, yielding a pellet of the low-density microsome (LDM) fractions. For western blotting, 10 μg of each membrane fraction was solubilized in sample buffer (2.3 M urea, 1.5% (w/v) SDS, 15 mM Tris/HCl and 100mM dithiothreitol, pH 6.8) at room temperature for 30 min, subjected to SDS/PAGE, and transferred to nitrocellulose membranes. The nitrocellulose membranes were immunoblotted with anti-GLUT4 antibody, and detected with enhanced chemiluminescence as described previously (Wang et al. 2006).

Ex vivo insulin signaling studies in isolated adipocytes

Isolated adipocytes were incubated for 30 min with 0 nM (basal), 10 nM, 50 nM and 100nM insulin, respectively, in Krebs-Ringer buffer containing 3% BSA. Adipocytes were then harvested for immunoprecipitation and immunoblot analysis of insulin signaling proteins. Because of the low abundance of IRS1 protein in mouse adipose tissue, ELISA assays were performed to compare total IRS1 protein levels in TH and B6 mice.

Statistical analysis

All data are presented as means ± SE. The statistical analyses were conducted in StatView (v. 4.5; Abacus Concepts, Berkeley, CA). The differences between two groups was assessed by Student's t-test, $p < 0.05$ was considered statistically significance.

Results

Reduced Glucose Transport in TH Mice

In comparison to B6 mice, adipocytes from TH mice displayed comparable basal but significantly reduced insulin stimulated 2-deoxyglucose uptake (Fig.1, 12% reduction under basal conditions and 60% reduction after insulin stimulation). The decrease in glucose uptake by adipocytes from TH vs B6 correlated with a significant 20% reduction in both basal and insulin-stimulated cellular GLUT4 content (Fig 2A) as determined by western blot analysis of whole adipocyte lysates, and a diminished localization of the GLUT4 protein at the adipocyte cell surface as assessed by immunofluorescence in adipose tissue (Fig 2C).

To further explore the mechanism of impaired glucose uptake in TH mice, we carried out a fractionation of the cellular membranes of adipocytes from B6 and TH mice. In un-stimulated adipose tissue of control B6 mice, 10% of GLUT4 was located at the cell surface in the plasma membrane (PM) and > 90 % in intracellular compartments, low-density microsomal (LDM)

and high-density microsomal (HDM) fractions. As expected, insulin treatment (0.5 U/kg) of B6 adipocytes resulted in 2.5-fold increased GLUT4 protein in the plasma membrane (PM) fraction along with a 30% decrease of GLUT4 protein in the low-density microsome (LDM) fraction, reflecting the translocation from the intracellular pools of GLUT4 transporter protein to the PM. In TH mice, in concordance with the reduction of total GLUT4 protein content, the combined membrane fraction (PM, LDM and HDM) GLUT4 showed approximately a 20% decrease compared to B6 controls (quantitation not shown). GLUT4 levels in the PM fraction slightly increased from basal levels after insulin stimulation. GLUT4 content in the low-density microsome fraction from TH mice after insulin stimulation remained unchanged (Fig 2B), reflecting an impairment of GLUT4 transport in adipose tissue of TH mice.

Histologically, adipose tissue from fasted B6 mice exhibited a punctate, non-linear cytoplasmic GLUT4 immunofluorescence as well as a weak immunofluorescence associated with the plasma membrane in the basal state (Fig 2C top left panel). GLUT4 immunofluorescence was redistributed from the condensed cytoplasmic staining to the plasma membrane after treatment with insulin and glucose in B6 mice (Fig 2C bottom left panel). GLUT4 staining in TH mice showed a similar distribution as B6 in the basal state but with less staining of the plasma membrane (Fig 2C top right panel). However, in TH mice treated with insulin and glucose the localization of GLUT4 remained unchanged, with the immunofluorescence signal in punctate staining in the cytoplasm with little signal present on the cell membrane (Fig 2C bottom right panel).

Impaired Insulin Signaling in TH Mice

Binding of insulin to its receptor results in auto-phosphorylation of the intracellular domain of the receptor. The phosphorylated receptor associates with IRS1, phosphorylated IRS1 binds and activates the lipid kinase phosphatidylinositol (PI) 3-kinase (PI3K) and triggers GLUT4 translocation and insulin stimulated glucose uptake (Buren, et al. 2002). We found that basal PI3K activity in adipose tissue of TH was lower than in B6, although not significantly so. Stimulation of PI3K activity by insulin was significantly reduced in TH mice (Fig. 3A). The association of the PI3K regulatory subunit p85 with IRS1 was markedly less in adipose tissue of TH mice. IRS1 binding to PI3K in TH was reduced both before (B6: 50.0±0.3% vs TH: 10.0 ±3.2%, $p<0.01$) and after insulin stimulation (B6: 100.0±8.6% vs TH: 8±3.6%, $p<0.01$) (Fig. 3B).

Decreased levels of IRS protein have been reported in insulin-resistant subjects as well as diabetic patients (Carvalho et al. 1999). We measured the protein and phosphorylation levels of IRS1 in TH mice by western blotting. IRS1 protein levels in adipose tissue of TH mice were significantly reduced compared to B6 in both basal and insulin stimulated states (Fig. 4A). The reduction of IRS1 protein was paralleled by a similar reduction in IRS1 tyrosine phosphorylation (Fig. 4B).

Since *Irs1* mRNA levels were not different between B6 and TH adipose tissue as measured by real time PCR (data not shown), we considered protein degradation as a mechanism for the reduced IRS1 levels in TH mice. IRS1 degradation is mediated by the proteasome degradative pathway and is primed by phosphorylation of serine residues on IRS1, particularly Ser307 (Gual, et al. 2005). In total protein lysates, the level of IRS1 phosphorylated at Ser307 was significantly lower in TH mice in the basal state and significantly higher after insulin stimulation compared to B6 (Fig. 4C left panel). However, importantly, the fraction of total IRS1 protein that was phosphorylated at Ser307 was higher in TH mice compared to B6 both in the basal state (1.5 fold) as well as after insulin stimulation (17 fold, Fig. 4C right panel).

To determine whether the defects of IRS1 in adipocytes of TH mice are intrinsic to adipose tissue or caused by the systemic metabolic milieu, we examined IRS1 protein levels and

tyrosine phosphorylation in primary-culture adipocytes derived from TH and B6 mice. Similar results compared to the in vivo data were obtained. Insulin increased total IRS1 protein in both B6 and TH mice in a concentration-dependent manner, however, to a lesser degree in TH (25% reduction in basal level and 40% reduction after 10 nM insulin stimulation, Supplementary Figure 1 A, ELISA and Figure 1 B, western blot). High insulin concentrations (100 nM) markedly suppressed IRS1 protein in both TH mice and B6 controls (Supplementary Figure 1 A). Similar results were observed in T2D patients (Rondinone, et al. 1997) Although tyrosine phosphorylation of IRS1 was similar in TH and B6 without insulin, in contrast to B6 derived adipocytes, insulin at 10 and 50 nM failed to stimulate IRS1 tyrosine phophorylation in TH adipocytes (Supplementary Figure 1 C).

Activation of JNK has been implicated in phosphorylating the IRS1 Ser307 residue in insulin resistant mice (Ozcan, et al. 2006). JKN1/2 activation [pTpY183/185] was measured and shown to be 1.5-fold higher in the basal state, and 2-fold higher after insulin stimulation in adipose tissue from TH mice compared to B6 controls (Fig 5A).

Co-localization of IRS1 and the 20S Proteasome Subunit, and Degradation of IRS1

Targeting of many proteins for proteasomal degradation is mediated by their modification with polyubiquitin. To assess whether the reduction of IRS1 was associated with enhanced degradation, immunoprecipitation with antibodies against ubiquitin and subsequent western blot analysis of the precipitate with anti IRS1 antibodies was performed. The decrease in IRS1 content due to degradation is associated with retarded migration of the protein band during SDS PAGE (Potashnik, et al. 2003). In agreement with this, a higher molecular weight IRS1-immunreactive band was observed in adipose tissue from TH mice but not in B6 (Fig 5B).

Suppressor of cytokine signaling 1 (SOCS1) has previously been shown to bind IRS1 protein and promote its ubiquitination and subsequent degradation (Rui, et al. 2002), and expression of SOCS proteins has been reported to be elevated in rodent genetic models of obesity and diabetes. SOCS1 protein levels were significantly higher in TH mice compared to B6 (~1.7-fold, Fig. 5C). SOCS1 localizes to the complex-associated 20S proteasome (Vuong, et al. 2004). To obtain cellular evidence for proteasomal targeting of IRS1, we stained adipose tissue samples from B6 and TH mice for the 20S core alpha and beta subunits of the proteasome. The 20S alpha and beta subunits of the proteasomes were localized throughout the cytoplasm of B6 adipocytes as shown Fig. 6A. In TH adipose tissue considerably more punctate staining for proteasomal structures was observed (Fig. 6A). In contrast to B6 where IRS1 staining was observed in the nucleus and cytoplasm (Fig. 6B. top panel), in TH mice IRS1 staining colocalized with staining for the 20S subunit in cytoplasmic proteasomal structures (Fig. 6B. bottom panel).

Discussion

Previously we have described a new mouse model for T2D, the inbred TALLYHO/Jng (TH) strain. TH mice are moderately obese, hyperinsulinemic, glucose intolerant, and insulin resistant (Kim et al. 2001),(Kim et al. 2006). Although occasionally diabetic females are observed in our colony, hyperglycemia is largely male limited as is typical for mouse models of T2D (Leiter, et al. 1991),.

The insulin resistance of T2D mellitus leads to a blunting of the insulin-stimulated increase in glucose uptake into fat and muscle. In muscle, this is due to defective stimulation of the translocation of the insulin sensitive glucose transporter, GLUT4 from intracellular storage pools to the cell surface (Watson, et al. 2004) (Shepherd and Kahn 1999). In adipocytes, the decreased insulin sensitivity is due to both this defect in insulin-stimulated translocation, as well as to decreased expression of GLUT4 (Watson et al. 2004) (Shepherd and Kahn 1999)

(Minokoshi et al. 2003). Reduced adipocyte GLUT4 protein levels have also been found in human obesity and T2D, as well as in numerous rodent models of insulin resistance (Shepherd and Kahn 1999). We previously had shown that there was a slight, but not significant reduction of GLUT4 content in soleus muscle from TH male mice (Kim et al. 2006). In the current studies, we found that there was 20% reduction in the total GLUT4 content in adipose tissue from TH compared to B6 mice. Importantly, GLUT4 content in the plasma membrane fraction and the low-density microsome (LDM) fraction in TH mice after insulin stimulation remained unchanged (Fig 2B), reflecting an impairment of GLUT4 transport in adipose tissue of TH mice.

IRS1 is required for normal induction of the signaling pathway that is key to many of the metabolic actions of insulin. Induction of IRS1 (3-fold) in rodents occurs within 20 min to 40 min following feeding or insulin injection (Bruning et al. 1997) (Ruiz-Alcaraz, et al. 2005). The induction is not due to changes in post-translational phosphorylation, but related to increased protein synthesis (Ruiz-Alcaraz et al. 2005). This short term insulin stimulation of IRS1 is also observed in human muscle (Ruiz-Alcaraz et al. 2005). After prolonged insulin exposure (4-48h), or in insulin resistant states a reduction in IRS1 levels is observed (Renstrom, et al. 2005). In the present studies, IRS1 content in TH adipose tissue is significantly lower than in B6 controls ($p<0.001$, Fig. 4A). In both strains of mice insulin leads to a significant induction of IRS1 protein, however to a lesser degree in TH compared to B6 (~ 2-fold vs 4-fold, respectively).

The GLUT4 translocation defect in adipose tissue could be ascribed to reduced levels of IRS1 in adipocytes, which consequently cause alterations in the phosphorylation status, and the activity of intermediates in the insulin signaling pathway through PI3 kinase in TH mice. The lower levels of IRS1 and reduced insulin signaling explain at least in part the insulin resistance observed in the TH model. It makes TH an attractive model for diabetes research since similar defects have been observed in human patients with T2D (Rondinone et al. 1997).

Our data showed an increase in serine phosphorylation and a decrease in tyrosine phosporylation of IRS1 in the insulin resistant TH mice compared to the more insulin sensitive B6 controls. While the phosphorylation of IRS1 on tyrosine residues is required for insulin-stimulated responses, the role of serine phosphorylation of IRS1 is primarily to terminate the insulin effects (Kim, et al. 1999). Increased serine phosphorylation (Ser307) of IRS1 was also reported in other models of insulin resistance in mice (Rui et al. 2002), (Ueki, et al. 2004), (Hirosumi et al. 2002). Gual et al and others have shown that stimulation with insulin increases the phosphorylation of Ser307 (mouse) in IRS1 (Gual, et al. 2003). Further more, Morino et al. found that in insulin resistant offspring of T2D parents reduced muscle glucose uptake was associated with increased IRS1 Ser312 (human) phosphorylation (Morino, et al. 2005). Bikman et al. found that in morbidly obese gastric bypass surgery patients increased IRS1 Ser312 phosphorylation was associated with insulin resistance which improved after surgery accompanied by a lowering of IRS1 Ser312 phosphorylation (Bikman, et al. 2008). The argument has been raised that phosphorylation of IRS1 at Ser312 (human)/ Ser307 (mouse) following insulin stimulation may be a physiologically normal response, possibly implicated in the determination of the correct amplitude and length of insulin action (Frojdo, et al. 2009).

One key signaling mechanism through which IRS1 can become phosphorylated at Ser307 (mouse)/Ser312(human) is the stress and inflammatory response pathway mediated by c-Jun N-terminal kinase (JNK1/2). As observed in dietary obesity and the *Lep*^{ob} model (Hirosumi et al. 2002), we find significant more activation of JNK1/2 in the TH model compared to B6 controls. Since JNK can be activated by free fatty acids (FFA) (Nguyen, et al. 2005), the elevated FFA levels in TH mice may play a role (Kim et al. 2001) (Kim et al. 2006).

Hyperphosphorylation of IRS1 on serine/threonine residues after chronic stimulation with insulin results in its targeted degradation by the proteasome (Rice, et al. 1993), (Sun, et al. 1999). Important mediators in this process are the SOCS proteins (Howard and Flier 2006), which target IRS1 and IRS2 for proteasomal degradation via an interaction with their SOCS box (Emanuelli, et al. 2001), (Ueki et al. 2004), (Rui et al. 2002). Higher levels of SOCS1 in TH mice suggest that the low IRS1 levels and concomitant insulin resistance in TH mice are at least in part due to SOCS mediated degradation of IRS1.

Degradation of IRS1 as a cause for insulin resistance in TH mice is also supported by our finding of IRS1 colocalization with proteasomal structures in TH mice, but not in B6. It had been described that polyubiquitin chains are essential for proteolytic targeting, whereas mono-ubiquitination might only affect sub-cellular localization (Beal, et al. 1996). Polyubiquitination, as found for IRS1 in TH mice (Fig 5B), cellular localization (Fig 6B), and reduced protein levels of IRS1 (Fig 4A) are, therefore, consistent with IRS1 being targeted for proteasomal degradation, leading to the insulin resistance observed in TH mice.

The impaired glucose tolerance and reduced glucose uptake in muscle and fat of TH mice are a plausible consequence of lower insulin signaling due to low IRS1 levels. This correlates well with findings in humans that low IRS1 expression and protein levels are predictive of insulin resistance and T2D (Carvalho et al. 1999). However, the cause for the IRS1 abnormalities including the potentially initiating event of JKN1/2 activation in TH mice as well as other models and humans remain to be determined. Nevertheless, the similarity of events leading to impaired glucose uptake and insulin resistance in the polygenic TH mouse with mechanisms proposed to mediate human type 2 diabetes makes TH an excellent model for investigating type 2 diabetes in general.

Supplementary Material

Refer to Web version on PubMed Central for supplementary material.

Acknowledgments

We thank Lawrence J. Bechtel and Elizabeth Hinman for technical assistance, and Dr. Edward H Leiter for reviewing the manuscript. We thank Jesse Hammer for assistance in preparing illustrations.

Funding The Jackson Laboratory core services were supported by an institutional grant (CA-24190). This work was supported by National Institute of Diabetes, Digestive and Kidney Diseases Grant DK-46977 (JKN).

References

Abel ED, Peroni O, Kim JK, Kim YB, Boss O, Hadro E, Minnemann T, Shulman GI, Kahn BB. Adipose-selective targeting of the GLUT4 gene impairs insulin action in muscle and liver. Nature 2001;409:729–733. [PubMed: 11217863]

Araki E, Lipes MA, Patti ME, Bruning JC, Haag B 3rd, Johnson RS, Kahn CR. Alternative pathway of insulin signalling in mice with targeted disruption of the IRS-1 gene. Nature 1994;372:186–190. [PubMed: 7526222]

Beal R, Deveraux Q, Xia G, Rechsteiner M, Pickart C. Surface hydrophobic residues of multiubiquitin chains essential for proteolytic targeting. Proc Natl Acad Sci U S A 1996;93:861–866. [PubMed: 8570649]

Bikman BT, Zheng D, Pories WJ, Chapman W, Pender JR, Bowden RC, Reed MA, Cortright RN, Tapscott EB, Houmard JA, et al. Mechanism for improved insulin sensitivity after gastric bypass surgery. J Clin Endocrinol Metab 2008;93:4656–4663. [PubMed: 18765510]

Bruning JC, Winnay J, Bonner-Weir S, Taylor SI, Accili D, Kahn CR. Development of a novel polygenic model of NIDDM in mice heterozygous for IR and IRS-1 null alleles. Cell 1997;88:561–572. [PubMed: 9038347]

Buren J, Liu HX, Jensen J, Eriksson JW. Dexamethasone impairs insulin signalling and glucose transport by depletion of insulin receptor substrate-1, phosphatidylinositol 3-kinase and protein kinase B in primary cultured rat adipocytes. Eur J Endocrinol 2002;146:419–429. [PubMed: 11888850]

Carvalho E, Jansson PA, Axelsen M, Eriksson JW, Huang X, Groop L, Rondinone C, Sjostrom L, Smith U. Low cellular IRS 1 gene and protein expression predict insulin resistance and NIDDM. FASEB J 1999;13:2173–2178. [PubMed: 10593864]

Emanuelli B, Peraldi P, Filloux C, Chavey C, Freidinger K, Hilton DJ, Hotamisligil GS, Van Obberghen E. SOCS-3 inhibits insulin signaling and is up-regulated in response to tumor necrosis factor-alpha in the adipose tissue of obese mice. J Biol Chem 2001;276:47944–47949. [PubMed: 11604392]

Farese RV, Sajan MP, Yang H, Li P, Mastorides S, Gower WR Jr, Nimal S, Choi CS, Kim S, Shulman GI, et al. Muscle-specific knockout of PKC-lambda impairs glucose transport and induces metabolic and diabetic syndromes. J Clin Invest 2007;117:2289–2301. [PubMed: 17641777]

Frojdo S, Vidal H, Pirola L. Alterations of insulin signaling in type 2 diabetes: a review of the current evidence from humans. Biochim Biophys Acta 2009;1792:83–92. [PubMed: 19041393]

Gual P, Gremeaux T, Gonzalez T, Le Marchand-Brustel Y, Tanti JF. MAP kinases and mTOR mediate insulin-induced phosphorylation of insulin receptor substrate-1 on serine residues 307, 612 and 632. Diabetologia 2003;46:1532–1542. [PubMed: 14579029]

Gual P, Le Marchand-Brustel Y, Tanti JF. Positive and negative regulation of insulin signaling through IRS-1 phosphorylation. Biochimie 2005;87:99–109. [PubMed: 15733744]

He W, Ikeda S, Bronson RT, Yan G, Nishina PM, North MA, Naggert JK. GFP-tagged expression and immunohistochemical studies to determine the subcellular localization of the tubby gene family members. Brain Res Mol Brain Res 2000;81:109–117. [PubMed: 11000483]

Hirosumi J, Tuncman G, Chang L, Gorgun CZ, Uysal KT, Maeda K, Karin M, Hotamisligil GS. A central role for JNK in obesity and insulin resistance. Nature 2002;420:333–336. [PubMed: 12447443]

Howard JK, Flier JS. Attenuation of leptin and insulin signaling by SOCS proteins. Trends Endocrinol Metab 2006;17:365–371. [PubMed: 17010638]

Hu Y, Liu Y, Pelletier S, Buchdunger E, Warmuth M, Fabbro D, Hallek M, Van Etten RA, Li S. Requirement of Src kinases Lyn, Hck and Fgr for BCR-ABL1-induced B-lymphoblastic leukemia but not chronic myeloid leukemia. Nat Genet 2004;36:453–461. [PubMed: 15098032]

Kim JH, Sen S, Avery CS, Simpson E, Chandler P, Nishina PM, Churchill GA, Naggert JK. Genetic analysis of a new mouse model for non-insulin-dependent diabetes. Genomics 2001;74:273–286. [PubMed: 11414755]

Kim JH, Stewart TP, Soltani-Bejnood M, Wang L, Fortuna JM, Mostafa OA, Moustaid-Moussa N, Shoieb AM, McEntee MF, Wang Y, et al. Phenotypic characterization of polygenic type 2 diabetes in TALLYHO/JngJ mice. J Endocrinol 2006;191:437–446. [PubMed: 17088413]

Kim YB, Nikoulina SE, Ciaraldi TP, Henry RR, Kahn BB. Normal insulin-dependent activation of Akt/protein kinase B, with diminished activation of phosphoinositide 3-kinase, in muscle in type 2 diabetes. J Clin Invest 1999;104:733–741. [PubMed: 10491408]

Krook A, Kawano Y, Song XM, Efendic S, Roth RA, Wallberg-Henriksson H, Zierath JR. Improved glucose tolerance restores insulin-stimulated Akt kinase activity and glucose transport in skeletal muscle from diabetic Goto-Kakizaki rats. Diabetes 1997;46:2110–2114. [PubMed: 9392506]

Leahy JL. Pathogenesis of type 2 diabetes mellitus. Arch Med Res 2005;36:197–209. [PubMed: 15925010]

Leiter EH, Chapman HD, Falany CN. Synergism of obesity genes with hepatic steroid sulfotransferases to mediate diabetes in mice. Diabetes 1991;40:1360–1363. [PubMed: 1936598]

Liu ML, Gibbs EM, McCoid SC, Milici AJ, Stukenbrok HA, McPherson RK, Treadway JL, Pessin JE. Transgenic mice expressing the human GLUT4/muscle-fat facilitative glucose transporter protein exhibit efficient glycemic control. Proc Natl Acad Sci U S A 1993;90:11346–11350. [PubMed: 8248251]

McCarthy MI, Zeggini E. Genome-wide association scans for Type 2 diabetes: new insights into biology and therapy. Trends Pharmacol Sci 2007;28:598–601. [PubMed: 17997168]

Minokoshi Y, Kahn CR, Kahn BB. Tissue-specific ablation of the GLUT4 glucose transporter or the insulin receptor challenges assumptions about insulin action and glucose homeostasis. J Biol Chem 2003;278:33609–33612. [PubMed: 12788932]

Morino K, Petersen KF, Dufour S, Befroy D, Frattini J, Shatzkes N, Neschen S, White MF, Bilz S, Sono S, et al. Reduced mitochondrial density and increased IRS-1 serine phosphorylation in muscle of insulin-resistant offspring of type 2 diabetic parents. J Clin Invest 2005;115:3587–3593. [PubMed: 16284649]

Nguyen MT, Satoh H, Favelyukis S, Babendure JL, Imamura T, Sbodio JI, Zalevsky J, Dahiyat BI, Chi NW, Olefsky JM. JNK and tumor necrosis factor-alpha mediate free fatty acid-induced insulin resistance in 3T3-L1 adipocytes. J Biol Chem 2005;280:35361–35371. [PubMed: 16085647]

O'Rahilly S, Barroso I, Wareham NJ. Genetic factors in type 2 diabetes: the end of the beginning? Science 2005;307:370–373. [PubMed: 15662000]

Ozcan U, Yilmaz E, Ozcan L, Furuhashi M, Vaillancourt E, Smith RO, Gorgun CZ, Hotamisligil GS. Chemical chaperones reduce ER stress and restore glucose homeostasis in a mouse model of type 2 diabetes. Science 2006;313:1137–1140. [PubMed: 16931765]

Potashnik R, Bloch-Damti A, Bashan N, Rudich A. IRS1 degradation and increased serine phosphorylation cannot predict the degree of metabolic insulin resistance induced by oxidative stress. Diabetologia 2003;46:639–648. [PubMed: 12750770]

Rees DA, Alcolado JC. Animal models of diabetes mellitus. Diabet Med 2005;22:359–370. [PubMed: 15787657]

Renstrom F, Buren J, Eriksson JW. Insulin receptor substrates-1 and -2 are both depleted but via different mechanisms after down-regulation of glucose transport in rat adipocytes. Endocrinology 2005;146:3044–3051. [PubMed: 15845625]

Rice KM, Turnbow MA, Garner CW. Insulin stimulates the degradation of IRS-1 in 3T3-L1 adipocytes. Biochem Biophys Res Commun 1993;190:961–967. [PubMed: 8382493]

Rodbell M. Metabolism of Isolated Fat Cells. I. Effects of Hormones on Glucose Metabolism and Lipolysis. J Biol Chem 1964;239:375–380. [PubMed: 14169133]

Rondinone CM, Wang LM, Lonnroth P, Wesslau C, Pierce JH, Smith U. Insulin receptor substrate (IRS) 1 is reduced and IRS-2 is the main docking protein for phosphatidylinositol 3-kinase in adipocytes from subjects with non-insulin-dependent diabetes mellitus. Proc Natl Acad Sci U S A 1997;94:4171–4175. [PubMed: 9108124]

Rui L, Yuan M, Frantz D, Shoelson S, White MF. SOCS-1 and SOCS-3 block insulin signaling by ubiquitin-mediated degradation of IRS1 and IRS2. J Biol Chem 2002;277:42394–42398. [PubMed: 12228220]

Ruiz-Alcaraz AJ, Liu HK, Cuthbertson DJ, McManus EJ, Akhtar S, Lipina C, Morris AD, Petrie JR, Hundal HS, Sutherland C. A novel regulation of IRS1 (insulin receptor substrate-1) expression following short term insulin administration. Biochem J 2005;392:345–352. [PubMed: 16128672]

Shepherd PR, Kahn BB. Glucose transporters and insulin action--implications for insulin resistance and diabetes mellitus. N Engl J Med 1999;341:248–257. [PubMed: 10413738]

Storgaard H, Song XM, Jensen CB, Madsbad S, Bjornholm M, Vaag A, Zierath JR. Insulin signal transduction in skeletal muscle from glucose-intolerant relatives of type 2 diabetic patients [corrected]. Diabetes 2001;50:2770–2778. [PubMed: 11723060]

Sun XJ, Goldberg JL, Qiao LY, Mitchell JJ. Insulin-induced insulin receptor substrate-1 degradation is mediated by the proteasome degradation pathway. Diabetes 1999;48:1359–1364. [PubMed: 10389839]

Sung YY, Lee YS, Jung WH, Kim HY, Cheon HG, Yang SD, Rhee SD. Glucose intolerance in young TallyHo mice is induced by leptin-mediated inhibition of insulin secretion. Biochem Biophys Res Commun 2005;338:1779–1787. [PubMed: 16288988]

Tsuji Y, Kaburagi Y, Terauchi Y, Satoh S, Kubota N, Tamemoto H, Kraemer FB, Sekihara H, Aizawa S, Akanuma Y, et al. Subcellular localization of insulin receptor substrate family proteins associated with phosphatidylinositol 3-kinase activity and alterations in lipolysis in primary mouse adipocytes from IRS-1 null mice. Diabetes 2001;50:1455–1463. [PubMed: 11375348]

Ueki K, Kondo T, Kahn CR. Suppressor of cytokine signaling 1 (SOCS-1) and SOCS-3 cause insulin resistance through inhibition of tyrosine phosphorylation of insulin receptor substrate proteins by discrete mechanisms. Mol Cell Biol 2004;24:5434–5446. [PubMed: 15169905]

Vuong BQ, Arenzana TL, Showalter BM, Losman J, Chen XP, Mostecki J, Banks AS, Limnander A, Fernandez N, Rothman PB. SOCS-1 localizes to the microtubule organizing complex-associated 20S proteasome. Mol Cell Biol 2004;24:9092–9101. [PubMed: 15456882]

Wang Y, Seburn K, Bechtel L, Lee BY, Szatkiewicz JP, Nishina PM, Naggert JK. Defective carbohydrate metabolism in mice homozygous for the tubby mutation. Physiol Genomics 2006;27:131–140. [PubMed: 16849632]

Watson RT, Kanzaki M, Pessin JE. Regulated membrane trafficking of the insulin-responsive glucose transporter 4 in adipocytes. Endocr Rev 2004;25:177–204. [PubMed: 15082519]

Zisman A, Leibovici D, Kleinmann J, Siegel YI, Lindner A. Predicting CAP in patients with intermediate PSA using modified PSA indices. Can J Urol 2000;7:1144–1148. [PubMed: 11151095]

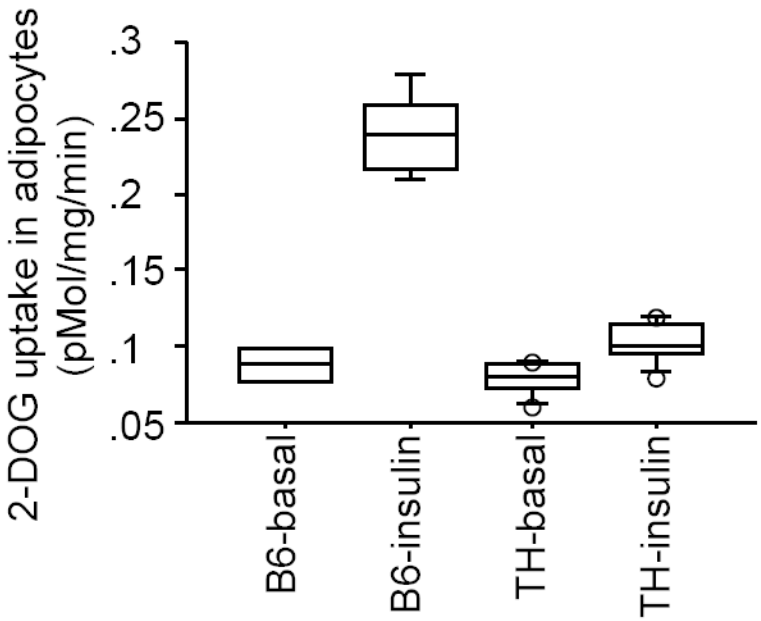

Figure 1.

Reduced glucose uptake in TH mice. Epididymal adipocytes were isolated from 10-wk-old TH mice (n=8-10 mice per group) as well as B6 controls (n=8 mice per group), and incubated in the absence or presence of insulin (70 nM) for 30 min. Glucose uptake was assessed by adding trace amounts of 2-[^{3}H]-deoxyglucose.

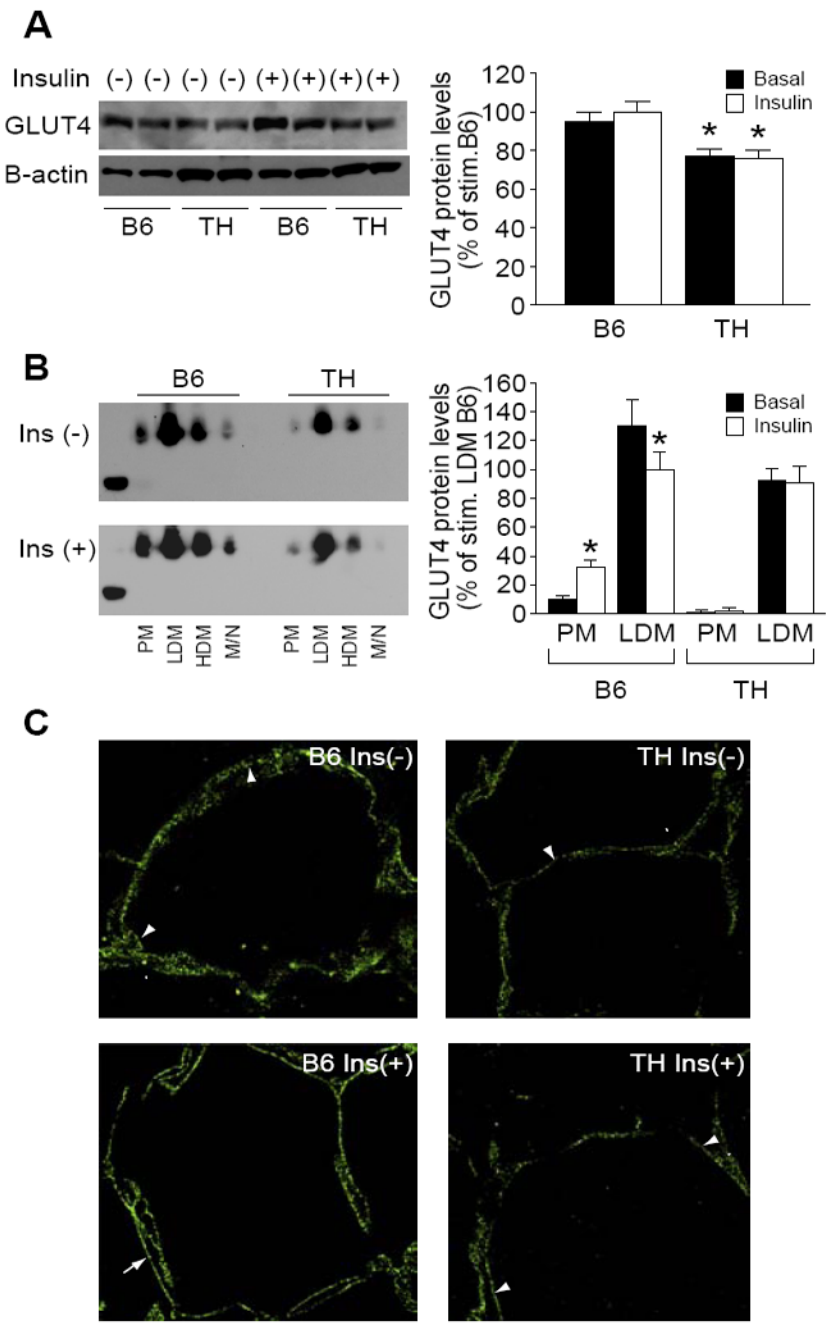

Figure 2.

Reduced GLUT4 translocation in TH mice. A. Western blot analysis of GLUT4 protein from adipose tissue in B6 and TH mice. B. Subcellular distribution of GLUT4 protein from adipocytes of B6 and TH mice. Plasma membrane (PM), low density microsome (LDM) and high density microsome (HDM) fractions were prepared from adipocytes treated with insulin or saline, and GLUT4 was detected by western blot as described in Materials and Methods (n=6 per group). Data from three experiments were quantitated by densitometry, and graphed relative to the value for insulin stimulated LDM B6 control, which was assigned a value of 100%.

C. Confocal fluorescent localization of adipocyte GLUT4 protein in B6 control mice (left panel) and TH mice (right panel). Mice were either fasted overnight and left untreated, Ins (-), or allowed to feed ad lib and given an intraperitoneal injection of insulin and glucose, Ins (+). Adipose tissue was cryopreserved. Arrowheads mark several locations of punctate cytoplasmic staining in adipocytes. Arrows mark locations of extensive membrane-associated GLUT4 in adipocytes of insulin stimulated B6 mice. Images are representative of three independent experiments (n=3 per group). *, $p < 0.05$ in fractions of PM and LDM different from basal versus respective insulin stimulated states.

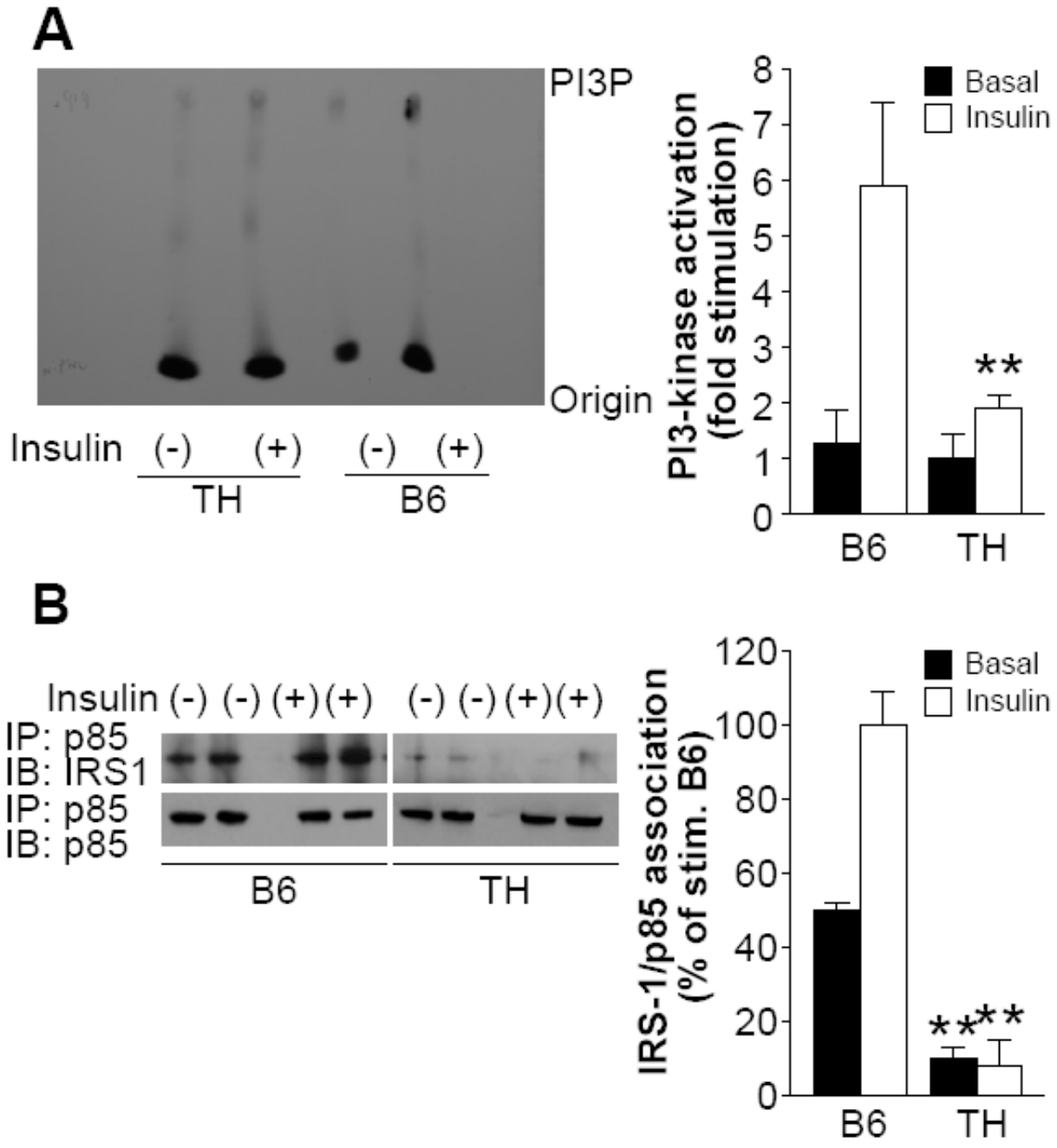

Figure 3.

Impaired insulin signaling in TH mice.

A. Impaired PI3K activity in adipose tissue of TH mice. Ten-week-old male mice (n=10-12 per group) were fasted overnight and given insulin (0.5U/kg) or saline. Adipocyte lysates were immunoprecipitated with anti-phosphotyrosine antibodies and immune complexes were assayed for their ability to phosphorylate phosphatidylinositol. Reaction products were resolved by thin layer chromatography, and results were quantified using a phospho-imager as described in Materials and Methods. B. Decreased association of p85 with IRS1 in TH mice. Adipose tissue was isolated from TH and control mice (n=10-12 per group) that were treated with insulin (0.5U/kg) or saline. Equal amounts of protein lysates (500μg) were

immunoprecipitated with anti-p85 antibody followed by western blot analyses with anti-IRS1. Membranes were stripped and re-probed with anti-p85 to confirm p85 levels. Data from three experiments were quantified by densitometry, and graphed relative to the value for insulin stimulated B6 control, which was assigned a value of 100%. **, P< 0.01 for TH samples versus the B6 samples in basal or insulin stimulation state, respectively.

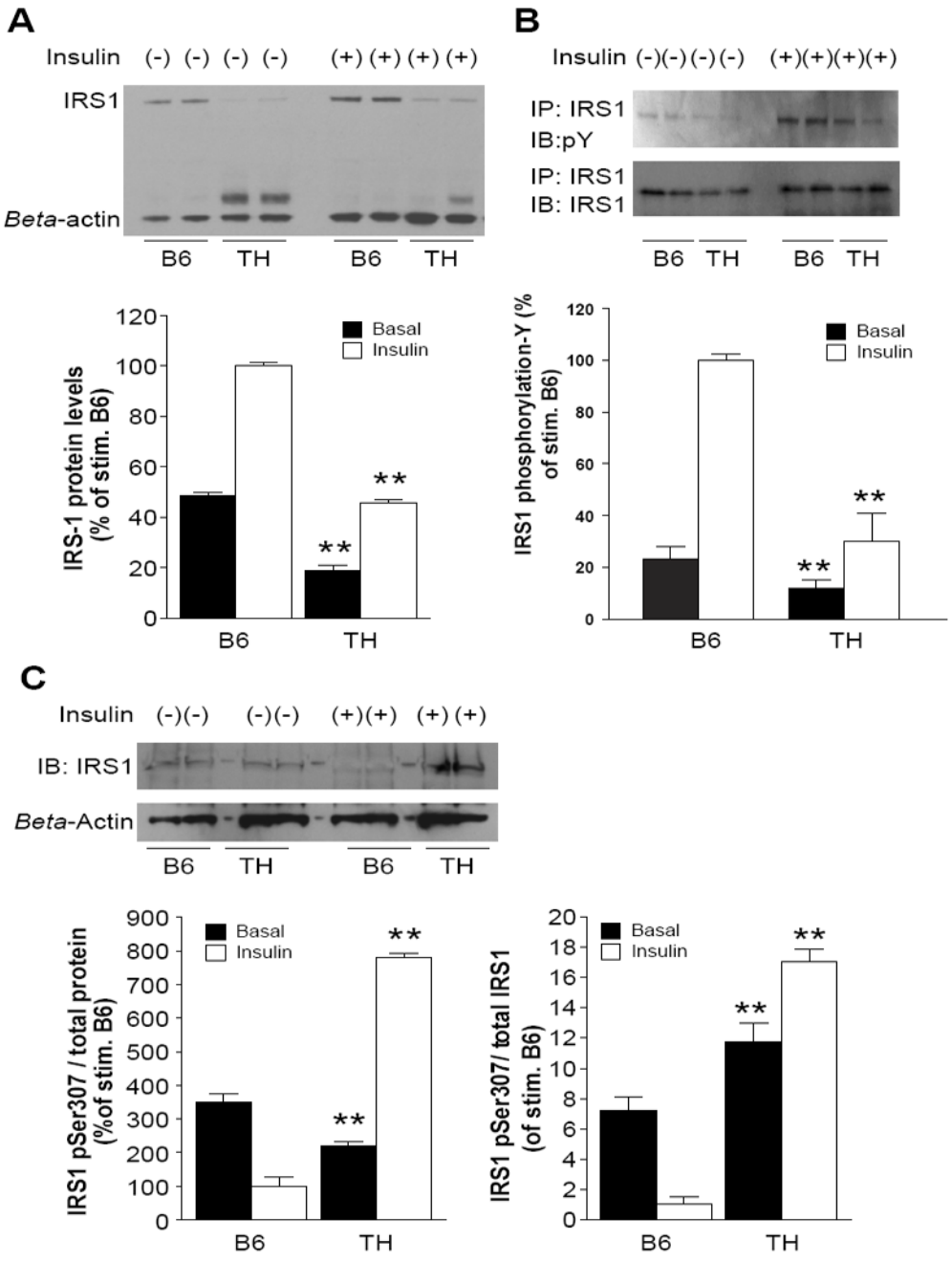

Figure 4.

Reduced levels of IRS1 protein and aberrant phosphorylation of IRS1 in TH mice.

A. Western Blot analysis of IRS1 protein from adipose tissue in B6 and TH mice. Animals (n=12 per group) were fasted overnight and then given insulin (0.5U/kg) or saline. Lysates (20 μg/ well) were resolved on a 3-8% polyacrylamide gradient Tris-Acetate gel, transferred to nitrocellulose and probed with anti-IRS1 antibody. Figures are representative of three independent experiments. B. Mice were fasted overnight and given insulin (0.5U/kg) or saline and adipocyte lysates were prepared for immunoprecipitation. Immunoprecipitates of IRS1 were probed for phosphotyrosine (P-Y) by immunoblotting (IB). Membranes were stripped and re-probed with anti-IRS1 to confirm IRS1 levels. C. Western Blot analysis of IRS1 S307

from adipose tissue lysates. IRS1pSer307 was measured as fraction of total protein lysates (left panel) and total IRS1 contents (right panel), respectively. Data from three experiments were quantified by densitometry, and graphed relative to the value for insulin stimulated B6 control. *, $p < 0.05$, **, $P< 0.01$ for TH samples versus the B6 samples in basal or insulin stimulation state, respectively.

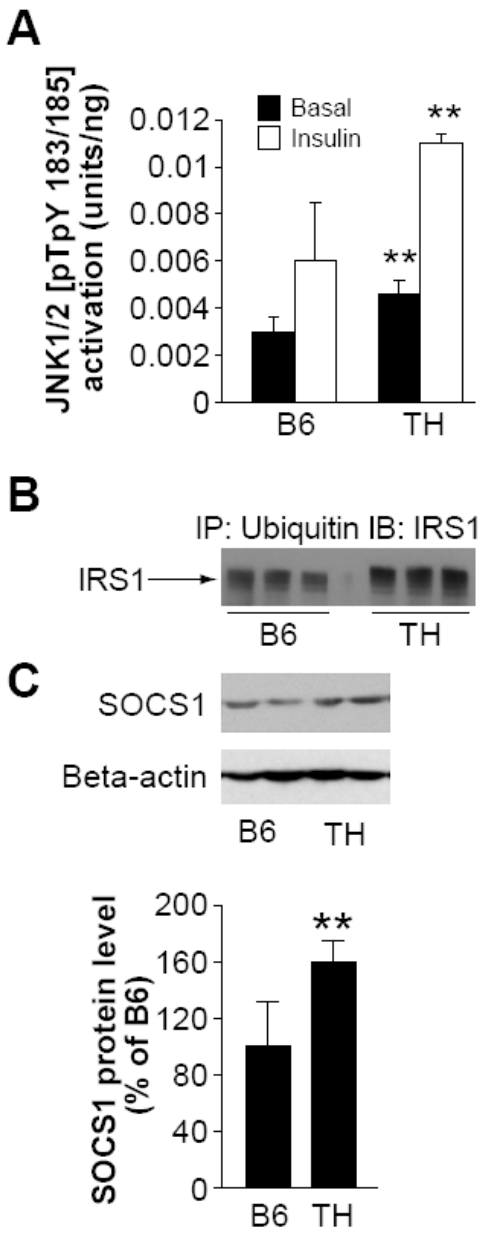

Figure 5.

Degradation of IRS1 protein from adipose tissue of TH mice.

A. Activation of JNK1/2[pTpY183/185] in adipose tissue of B6 and TH mice at 10 weeks of age (n=6-8). B. Immunoprecipitation with antibodies against ubiquitin and subsequent western blot analysis of the precipitate with anti-IRS1 antibodies showed increased amounts of polyubiquinated IRS1 in TH adipose tissue. C. Western Blot analysis of SOCS1 from adipose tissue lysates. Data from three experiments were quantified by densitometry, and graphed relative to the value for insulin stimulated B6 control, which was assigned a value of 100%. *, $p < 0.05$, **, $P< 0.01$ for TH samples versus the B6 samples in basal or insulin stimulation state, respectively.

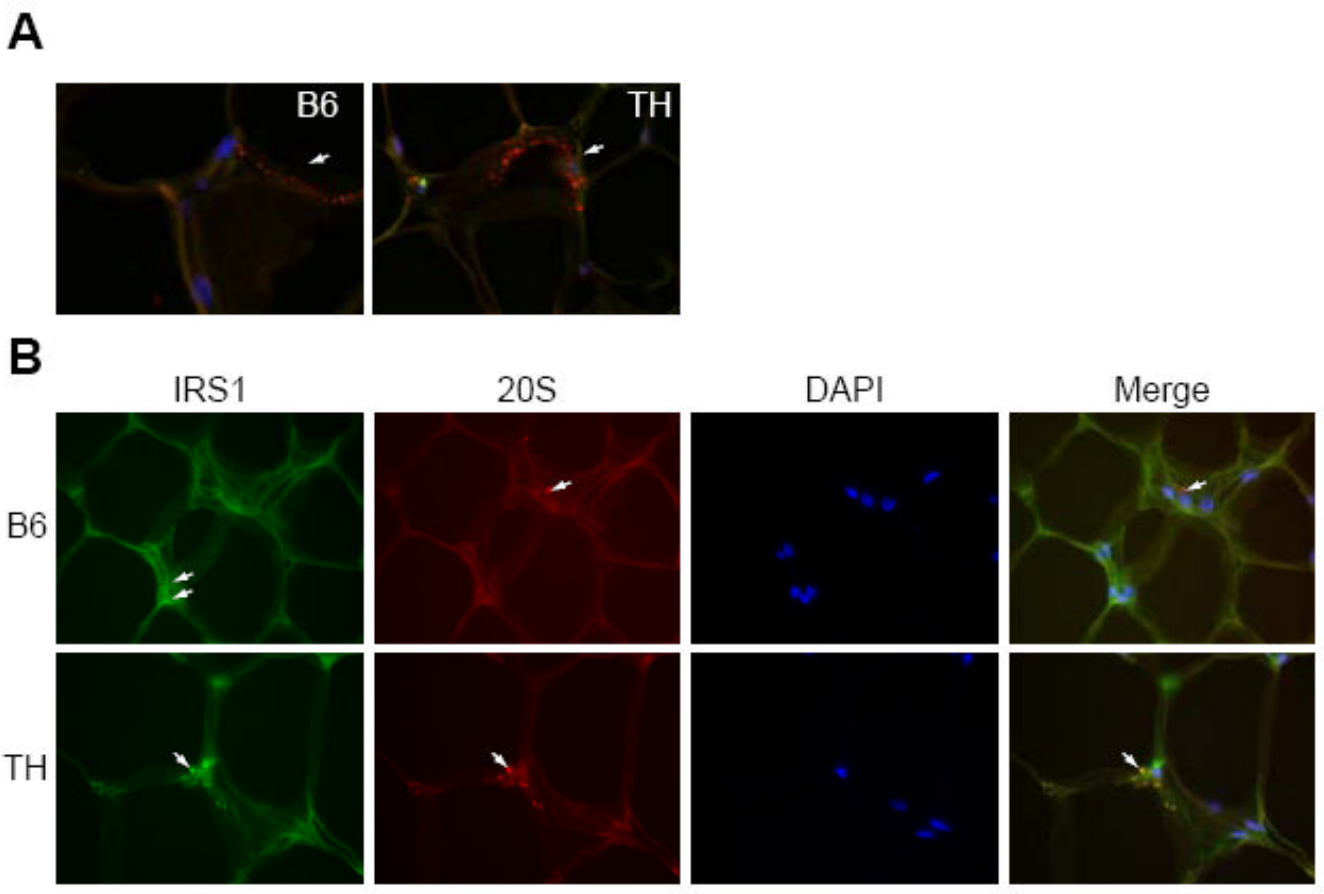

Figure 6.

Co-localization of IRS1 and the 20S proteasome subunit.

A. Adipose tissue was probed with antibodies against the 20S proteasome (red), and DAPI for DNA (blue). Arrows mark locations of 20S cytoplasmic staining in B6 and TH mice. B. Adipose tissue from TH and B6 mice was stained with antibodies against IRS1 (green) or against the 20S proteasome (red), or with DAPI for DNA (blue) and the pictures were merged in the last panel. Arrows mark different locations of IRS1 and 20S in B6 mice (top panel), arrows mark co-localization of IRS1 and 20S in TH mice (bottom panel).